Available online at www.sciencedirect.com

ScienceDirect

Procedia Engineering 89 (2014) 304 – 310

Procedia Engineering

www.elsevier.com/locate/procedia

16th Conference on Water Distribution System Analysis, WDSA 2014

Water Leakage Evolution Based On GPR Interpretations

D. Ayala-Cabrera[a,*], E. Campbell[a], E.P. Carreño-Alvarado[a], J. Izquierdo[a], R. Pérez-García[a]

[a]*FluIng-IMM, Universitat Politècnica de València, Camino de Vera s/n, Valencia, 46022, Spain*

Abstract

This document shows some aspects regarding water leakage time propagation through the underground, in controlled laboratory conditions, using a drilled PVC pipe, through the interpretation of GPR images. The extraction of relevant patterns is possible since GPR interpretations allow to obtain surfaces and volumes that can be easily identified by non-highly specialized personnel in the analysis of raw data. The results of this study are promising since they help promote the realization of techniques able to validate models for generation, distribution and prediction of water leaks in water supply systems using GPR as a non-destructive method.

Peer-review under responsibility of the Organizing Committee of WDSA 2014

Keywords: Water leakage evolution; ground penetrating radar; water supply systems; leak visualization; GPR interpretations .

1. Introduction

Nowadays, water leakage detection and control is one of the most challenging situations for network management in water supply systems (WSSs). This paper addresses the problem of leakage in WSSs from the perspective of non-destructive methods. Among the non-destructive techniques currently used to locate leaks in WSSs, the most popular are acoustic methods, infrared thermography, and ground penetrating radar (GPR) [5]. GPR has shown to be an effective non-destructive tool that favors inspection of WSSs by demarcating in GPR images (radargrams) contrasts between the leaked water and the surrounding area that are caused by differences in their dielectric characteristics [4]. In this sense, this work attempts to evaluate the feasibility of monitoring water leakage evolution in WSSs, through the use of GPR as a non-destructive method. To this purpose, laboratory tests were performed in which we seek to

* Corresponding author. Tel.: +34 963 877 007 ext. 86112;
E-mail address: daaycab@upv.es

Peer-review under responsibility of the Organizing Committee of WDSA 2014
doi:10.1016/j.proeng.2014.11.192

extract features of water leakage from GPR images. Temporal evolution of water leakage is a first feature evaluated in this work. The main idea is to produce reliable knowledge and robust data that promote the phenomenon comprehension, thus favoring the prediction and/or detection of water leakage in the system. The aim is to increase the models' approximation abilities, so as to improve operational and maintenance activities and favoring decision-making on WSSs management. This is possible because GPR interpretations enable to obtain surfaces and volumes that can be easily identified from data analysis by non-highly qualified personnel while using non-destructive methods.

In this paper water leak propagation through soil from a PVC pipe is addressed. This is performed using GPR images obtained under controlled laboratory conditions. The installed plastic pipe was selected considering the difficulty for identification of this material through the use of non-destructive methods [3], and the decreasing visibility of the surrounding objects caused by plastic materials [2].

Knowledge obtained with the methodology described in this paper may provide basic know-how to other engineering fields regarding such aspects as fluid dispersion through subsoil, infrastructure risks associated to water leaks, wet bulb distribution for irrigated areas, among others. In this sense, other interesting works show support to this line of research, for example, with the non-destructive methods for plume dispersion of contaminants [6], in the case of geophysical methods for delineating plumes caused by oil contamination through soil and groundwater. Also in [7] the pollution plumes evaluation in an urban environment is addressed.

The paper is organized as follows. In the first section, we have given a brief introduction. The second section presents the characteristics of the tests performed. The third section addresses GPR interpretations and classifications of the tests performed. The fourth section compiles the analysis of results. Finally, a section of conclusions closes the document.

2. Materials and Methods

This section presents the layout of the laboratory tests. For the set of tests performed, a pipe commonly used in WDSs is buried in dry soil in a tank. The characteristics of the buried pipe are: (a) PVC; (b) diameter of 100 mm; (c) length of 0.95 m; (d) hole drilled for simulating the leak in the central part of the pipe; (e) two points for water input and output with connections at the ends. A wooden tank measuring 1.0m × 1.0m × 0.60m was used. After the pipe was positioned, its supports were removed, and it was then covered with dry soil. The surface of the tank was covered with a polypropylene plate. Eleven paths parallel to the X-axis and another eleven paths parallel to the Y-axis were marked on this plate. These 22 paths were spaced 0.10m apart, thus forming the sampling grid. Three out of these 22 paths were chosen parallel to the pipe, and 1 in transversal direction. We term this layout *control set* (CS). The 3 parallel profiles are 400mm long and were placed from position (400,700) to position (400,300) for the CS_{sA} (Control Set, slice A), from (500,700) to (500,300) for the CS_{sB} (Control Set, slice B), and from (600,700) to (600,300) for the CS_{sC} (Control Set, slice C). The transversal profile was measured between position (900,500) and (200,500), giving the CS_{sD} (Control Set, slice D). The selection of these profiles was decided aiming at crossing the pipe in longitudinal (CS_{sC}) and transversal (CS_{sD}) directions, both profiles intersecting azimuthally above the leak point. The other two profiles were placed strategically close to the pipe and intended to keep trace of the leak. Onto each line of this mesh, the GPR antenna was slipped.

The GPR equipment used in each survey corresponds to a commercial monostatic antenna with a central frequency of 1.5 GHz. The parameters of the equipment correspond to 120 traces/s, 512 samples/trace and 20 ns/512 samples.

The total duration of the tests, corresponding to a time of 35 minutes, is divided into 3 phases (see Table 1). In Phase 1, the initial condition (corresponding to time zero), the test is performed under the established configuration with no water in the system. Phase 2 corresponds to the filling of the pipe. Times 2 and 3 correspond to a volume of water less than that required to fill the pipe. Phase 3, in turn, corresponds to the water added to the system once the pipe has been filled. The temporal distribution of the tests performed and the corresponding phase are shown in full in Table 1.

Table 1. Time measurement configuration for the GPR tests

Time	time (hh:mm:ss)	Phase
t0	00:00:00	Phase 1
t1	00:02:10	Phase 2
t2	00:06:02	Phase 2
t3	00:11:42	Phase 3
t4	00:14:02	Phase 3
t5	00:17:03	Phase 3
t6	00:21:54	Phase 3
t7	00:28:05	Phase 3
t8	00:33:06	Phase 3
t9	00:35:06	Phase 3

3. Interpretation and classification of the GPR profiles

This section presents the proposed process to extract the contours for the GPR images. This process consists of the following steps: a) contrast, b) identification of ranges where the objects of interest are placed, c) demarcation of boundaries, and d) manual classification of the boundaries. This process, based on a process described in [1], is described below.

In this document, a contrast with a reference image for each GPR profile obtained is considered. This is done in order for the objects of interest to be clearly visible. The main input of this work is the raw data obtained from the GPR, visualized as radargrams. The received signals are stored in a matrix MR (raw radargram matrix), which is composed of m-vectors b_k, k = 1,…, n (traces), which represents the change in depth of the electromagnetic properties of the ground. We will represent this matrix by columns: $MR = [b_1, b_2, \ldots, b_{n-1}, b_n]$. The length, m, of vector b_k, corresponds to the volume of data recorded in each track, which depends on the characteristics of the signal of the equipment used. The contrast matrix for each profile is given by $MC_{st} = abs([MR_{st}] - [MR_{s0}])$; s corresponds to the profile to contrast, its domain being {A, B, C, D}, and t is the measurement time, $t = 1, \ldots, 9$, (see Table 1). Time zero corresponds to the matrices obtained through the four profiles for the condition of absence of water in the system (Phase 1). The images obtained with these matrices are analyzed in detail in order to find ways to provide information of the buried pipe and its boundary conditions.

After several iterations, the best display for the leakage was found in a range of [120 1500] for slices A, [200 3000] for slices B, [300 3450] for slices C, and [320 3650] for cross sections (slices D). Within these ranges we proceeded to define the resulting shapes in the images. It should be noted that the forms obtained for each image with an area of less than 90 pixels were eliminated. This was done in order to facilitate the subsequent classification process and improve the visualization of the leak in the images. The process of manual classification was made based on the observation of all images. After observing all the pictures, it was decided that the easiest way to understand the images was by grouping the contours obtained into 4 groups for profiles A, B and C. For section D, in turn, a new group was taken into account. The 4 groups obtained were assigned a color scale, whose domain is {'gray', 'brown', 'cyan', 'red'}. For the additional profile obtained in group D, the extra color will be 'blue'. The criteria for classifying the areas were:

- ‘gray’: first area (in depth), with no relevant variation in the images
- ‘brown’: area after ‘gray’ (in depth), considerably varying during the last stages for all the profiles, delimiting from above the ‘cyan’ area
- ‘cyan’: area corresponding to the leaked water
- ‘red’: area that wraps the lower part of the ‘cyan’ area
- ‘blue’: this area, only clearly identified for profiles D, corresponds to the water within the pipe.

Although this process is carried out manually in this work, the goal is to carry it out automatically. This manual process may serve in future research to corroborate the results obtained by automatic extraction techniques. An example of the applied process is shown in Fig. 1. The aim is to improve the visualization in subsequent extraction and classification of contours.

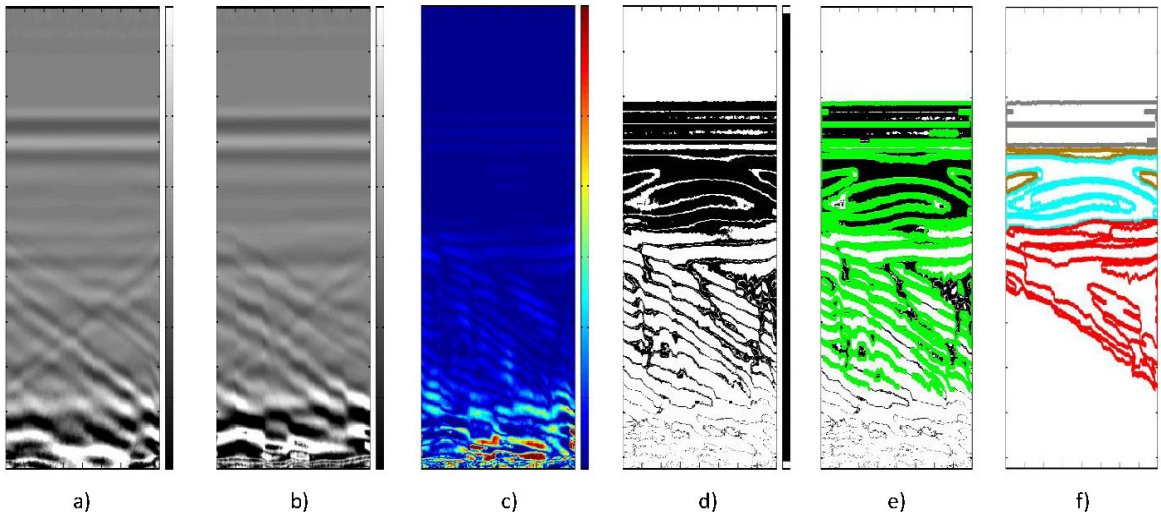

Fig. 1. (a) Raw slice, MR_{st} matrix; (b) white slice, MR_{s0}; (c) contrast matrix, MC_{st}; (d) selection of color range for the contrast matrix, (e) contours for the color range matrix, and (f) manual classification of the contours.

4. Analisis of results

The results obtained by applying the above described process of interpretation and classification are shown in Fig. 2 (sections A to C).

In Fig. 2, Phase 2 times (t1 and t2) are observed; a), b) and c) are not significantly different. This is consistent with the approach of the test, considering that this is the filling phase. The only difference between them lies in the depth displacement of the 'brown' area. This is the result of the introduction of water in the pipeline. Phase 3, for parts a) and b), shows correspondence to the form obtained for the leaked water. 'Cyan' areas are larger (comparing each time) in a) than in b), i.e. they are greater the further away from the leak point. In Phase 3, for part c), the 'cyan' area is observed only from t5 to t9. Since profile C corresponds to a longitudinal section of the pipe, this part corresponds to the leaked water that has risen by capillarity.

The results of application of the process of interpretation and classification for the D profiles are shown in Fig. 3.

In Fig. 3, Phase 2, the incremental area classified as 'blue' is observed, corresponding to the water inside the pipe. One can also observe that in the later times the area classed as 'cyan' begins to develop. This area reduces the visualization of the water contained in the interior of the pipe. This phenomenon has already been identified in a previous work [2], and corresponds to the visibility reduction of plastic pipes on GPR images due to the surrounding medium with greater reflection than the plastic pipe. However, Fig. 3 corroborates the previous classification of profiles A, B and C.

The variation of the forms in the various images enables to determine that it is possible to obtain to some extent the path of the water as it leaks from the pipe. While the results are not accurate and have some deformation, it is also true that they can be calibrated to establish a model of water leaked for each type of breakage, and relate the leak with the pressure and flow values in the system. Similarly, a more complete study with different soil types could serve to identify the type of propagation and to model the plume dispersion.

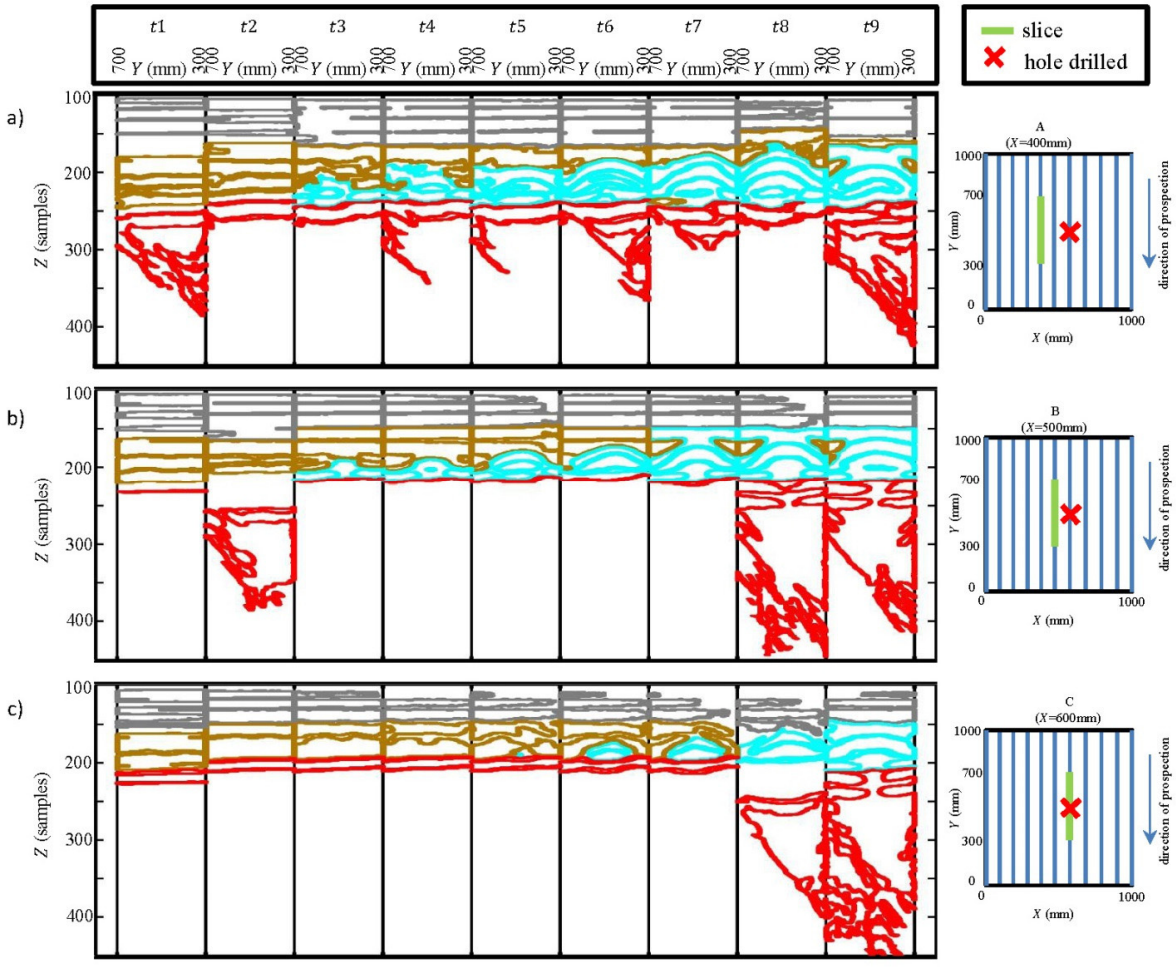

Fig. 2. (a-c) Interpretation and classification for the slices A to slices C

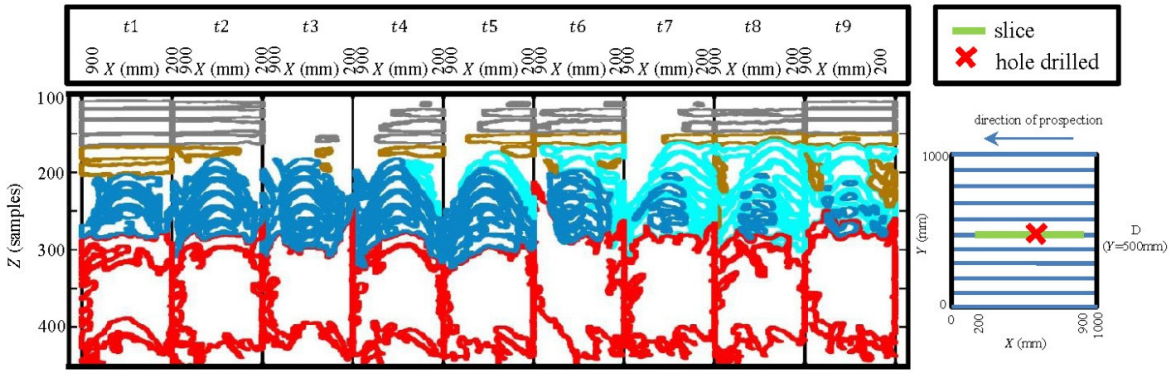

Fig. 3. Interpretation and classification for the slices D

To facilitate the visualization and understanding of the results, a fusion of the different classifications obtained was performed. Fusion of the shapes obtained from GPR images after the manual interpretation is performed by using 3D models (Fig. 4). This fusion was performed by positioning the points at their respective spatial coordinates and then plotting the end points of each group. These extreme points were connected by a Delaunay triangulation, which allowed visualization by way of surfaces.

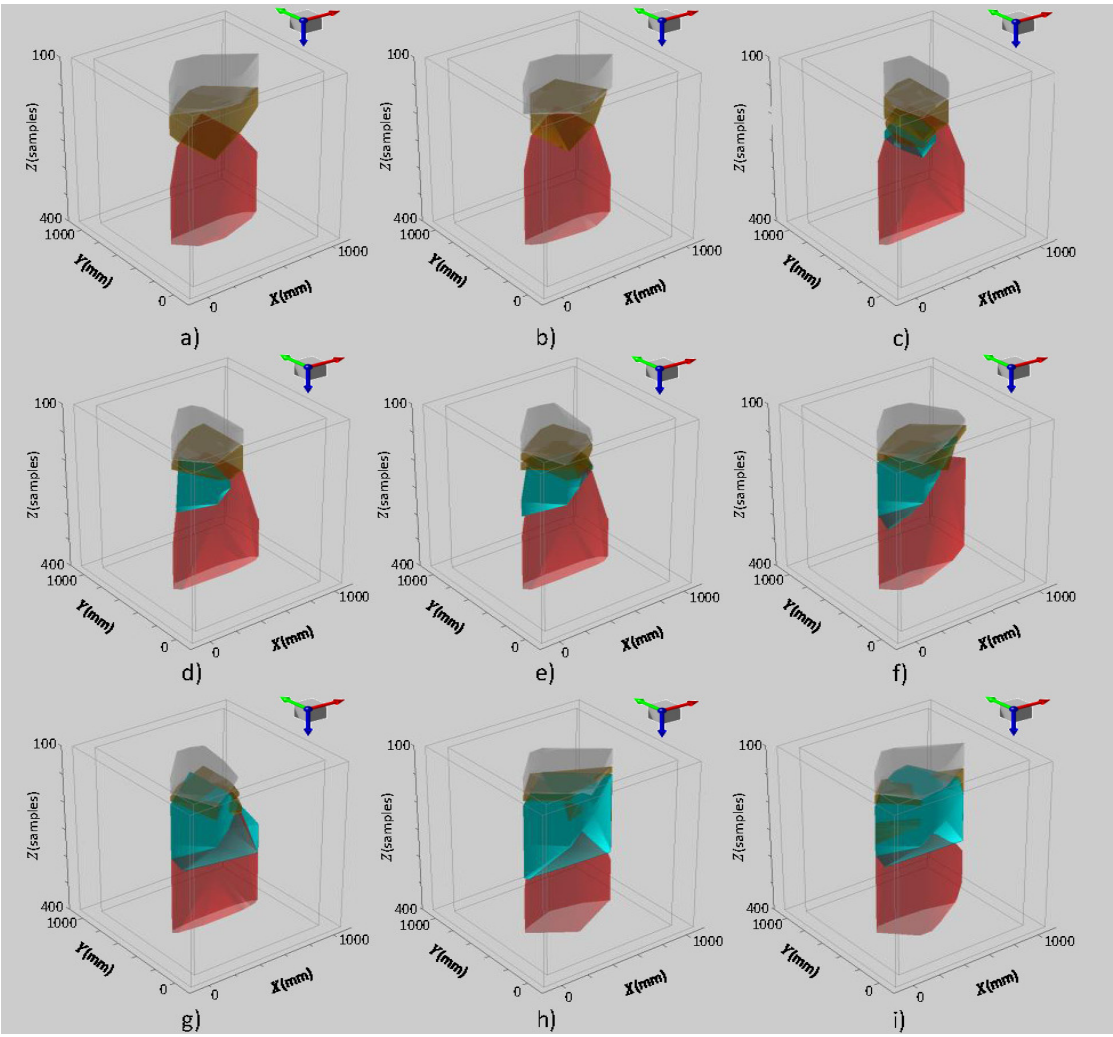

Fig. 4. Leak 3D evolution. (a-b) Phase 2, *t*1 and *t*2, respectively; (c-i) Phase3, *t3* till *t9*.

The blue area in Fig. 4 shows the water plum within the tank volume used, showing the difference between Phase 2 (Fig. 4, a) and b)) and Phase 3 (Fig. 4, c) to i)) trials. The variation of the volumes of the area of interest enables to determine the volume affected by the simulated water leak. In this way, the basis for generating theoretical dispersion models under more realistic conditions can be created. Similarly, the obtained 3D figures allow to non-highly qualified personnel to handle non-destructive techniques to better understand the phenomena of leakage and scattering of water in the soil.

5. Conclusions

Using the measurements, interpretations and fusion of interpretations of images of GPR described in this work we can conclude that it is feasible not only to detect, using non-destructive methods (in this case GPR), water in the subsoil, but to reconstruct the various stages of the leak, and to represent how water dissipates through the soil. Similarly, this work quantifies the volume of wet soil and the change of the volume in time. This produces more approximate models in terms of generation and/or detection of leakage.

In addition, this work shows the feasibility of monitoring anomalies over time through the use of non-destructive methods. Notably, even using very close measurements, as the parallel profiles used in this document, significant differences between the profiles may be found. This motivates to conduct further studies (using, for example, data mining methodologies) that allow the detection and location of these anomalies automatically. Furthermore, this study shows that it is possible to obtain forms beyond the classical hyperbolae, which may represent buried objects. This will undoubtedly facilitate the interpretation of these images by non-highly qualified personnel when using sophisticated tools and techniques such as GPR. Such is the case of water supply systems.

Acknowledgements

Part of this work has been developed under the support of an FPI (Formación de Personal Investigador)-UPV (Universitat Politècnica de València) scholarship granted to the first author by the Programa de Ayudas de Investigación y Desarrollo (PAID) of the Universitat Politècnica de València.

References

[1] D. Ayala-Cabrera, J. Izquierdo, S.J. Ocaña-Levario, R. Pérez-García, 2014. 3D Model construction of wáter supply system pipes base don GPR images. in: Proc. of 7th International Environmental Modelling and Software, San Diego, CA, USA, Daniel P. Ames, Nigel W.T. Quinn, Andrea E. Rizzoli (Eds.), 2014.

[2] D. Ayala-Cabrera, M. Herrera, J. Izquierdo, S.J. Ocaña-Levario, R. Pérez-García, GPR-based water leaks models in water distribution systems, Sensors, 13 (2013) 15912-15936.

[3] D. Ayala-Cabrera, M. Herrera, J. Izquierdo, R. Pérez-García, Location of buried plastic pipes using multi-agent support based on GPR images, J. Appl. Geophys., 75 (2011) 679–686.

[4] L. Crocco, F. Soldovieri, T. Millington, N.J. Cassidy, Bistatic Tomographic GPR imaging for incipient pipeline leakage evaluation, Prog. Electromagn. Res., 101 (2010) 307-321.

[5] S. Demirci, E. Yigit, I.H. Eskidemir, C. Ozdemir, Ground penetrating radar imaging of water leaks from buried pipes based on back-projection method, NDT&E Int., 47 (2012) 35-42.

[6] M. Moradi, M.K. Hafizi, B. Taheri, H.S. Kamal, Application of geophysical methods to delineation of LNAPL contaminated plume, in Proc. of the 7th IASME/WSEAS International Conference on Energy, Environment, Ecosystems and Sustainable Development and the 4th IASME/WSEAS International Conference on Landscape Architecture, Angers, 2011, pp. 135-139.

[7] P. Vaudelet, M. Schmutz, M. Pessel, M. Franceschi, R. Guérin, O. Atteia, A. Blondel, C. Ngomseu, S. Galaup, F. Rejiba, P. Bégassat, Mapping of contaminant plumes with geoelectrical methods. A case study in urban context, J. Appl. Geophys. 75 (2011) 738–751.